JOURNAL OF MATERIALS SCIENCE 28 (1993) 5909–5916

Effects of refined microstructures on ductility and toughness at room temperature in nickel-rich NiAl

TIANYI CHENG
Metal Materials Section, Beijing Institute of Technology, P.O. Box 327, Beijing 100081, People's Republic of China

Melt-spun Ni–34.6 at % Al ribbons with a minimum average grain size of 2.2 μm were prepared and the microstructures at room temperature were investigated. Refining the sizes of grains and other substructures resulted in interfaces of different types with very high density and uniform distribution. The reaction between the interfaces and propagating microcracks led to plastic deformation ahead of the crack tips and in larger regions with very fine grains, about 0.2 μm. Deflection, twisting and branching of the microcracks also resulted. The results indicate that the ductility and toughness of the nickel-rich NiAl all were considerably improved, which is consistent with previous test results. A simplified model based on the experimental results was used to analyse the mechanism of toughening NiAl. The important role of the interfaces in improving ductility and toughness of NiAl at room temperature is discussed.

1. Introduction

NiAl is of interest as a potential high-temperature structural material because of its many superior characteristics [1]. However, the severe brittleness of NiAl at room temperature is still a main problem for its application. Hence, following the original study by Schulson [2], much work [3–6] has been done in refining grain size to improve the poor ductility of NiAl. Schulson and Barker [3] reported that refining grains below a critical size is the key factor to enhance the ductility of NiAl. Chan [6] performed a theoretical calculation and claimed that the critical grain size for stoichiometric NiAl was about 2.8 μm. It was also pointed out recently [7] that discrepancies [8] with Schulson's work are just that the grain size of NiAl in the work [8] was much larger than the critical size. In fact, attempts to refine the grain size of NiAl have been limited by the traditionally cast process and the minimum grain size of NiAl in Schulson's work was 14 μm. Gaydosh *et al.* [4] manufactured NiAl ribbons using melt-spinning technology with a peripheral wheel speed of 20 $m\,s^{-1}$ but the minimum grain size (the width of the columnar grains) was 5.4 μm, which again was larger than the critical size, according to Chan's work [6] although the bend ductility of their ribbons was improved. On the other hand, in terms of structural application, the toughness of intermetallics such as NiAl is much more important than the ductility, although the toughness correlates closely with the ductility. Schulson and Barker [3] assumed that grain-size reduction can affect the fracture process, and Chan [6], based on his calculation, reported that refining grain to the critical size may have the beneficial effect of increasing the critical-stress strength factor, K_{1c}, and/or tearing modules. However, research into the mechanism of toughening NiAl by refining grain size and the relation between improvement of ductility and enhancement of toughness in NiAl, has been very sparse.

In the present work, the effects of refining sizes of microstructures on ductility and toughness at room temperature in a nickel-rich NiAl with a minimum average grain size of 2.2 μm was investigated, based on a study of the microstructures. The mechanism of toughening NiAl was specifically discussed.

2. Experimental procedure

The conventional induction-melting process was used to prepare a nickel-rich NiAl cast alloy from 99.999% pure nickel and aluminium in an argon atmosphere. The thin ribbons with a width of about 4 mm were then produced using a melt-spinning technique from the cast alloy. Different peripheral wheel speeds (Table I) were used to change the cooling rates. The ribbon composition was analysed using a chemical method and the actual composition of the ribbons was Ni–34.6 at % Al. The thickness and fracture surfaces of the ribbons were analysed using a Hitachi S-530 scanning electron microscope (SEM). A linear intercept method was employed to determine the grain sizes. The microstructures of the ribbons were examined using a Philips PA2000 X-ray diffractometer (XRD), Philips CM12, CM20 and Jeol-2000FX transmission electron microscopes (TEM).

3. Results

3.1. Refined microstructures

The ribbons consisted of martensite NiAl (M-NiAl) with the $L1_0$ structure and few remaining β-NiAl with

TABLE I Peripheral wheel speeds, v, average thicknesses, t, and grain sizes, d, of Ni–34.6 at % Al ribbons

Ribbons	v (m s^{-1})	t (μm)	d (μm)
N-1	47.1	14.7	2.2
N-2	39.2	24.4	3.1
N-3	27.5	30.3	5.3

the B2 structure, based on analysis by XRD and TEM [9]. The average grain sizes, d (Table I), of the ribbons were very small and decreased with increasing peripheral wheel speeds, v, and decreasing thickness, t, or increasing cooling rates. For ribbon N-3, v and d were nearly the same as that employed in Gaydosh *et al.*'s work ($v = 20$ m s^{-1}, $d = 5.4$ μm) [4]. The peripheral wheel speeds of ribbons N-1 and N-2 were larger so the cooling rates during rapid solidification were higher and the average grain sizes of the ribbons were smaller than that in their work.

Most of M-NiAl had a parallel lamellar-like twin or stacking fault structure with complex substructures of secondary twins or stacking faults. Fig. 1 shows the typical morphology of M-NiAl. The appearance of the grains was not regular and sometimes there were several variants with different orientations within one grain. The average thickness of the twin or stacking fault plates was very thin, about 60 nm and the average thickness of the secondary twin or stacking fault plates was much thinner, about 8 nm. Fig. 1b shows many parallel, very regular and step-like M-NiAl twin plates within a grain in ribbon N-1, in which the thickness of the secondary twin plates is only about 5 nm. The other type of twin M-NiAl with thin twin plates and its identification in ribbon N-3 are shown in Fig. 2. The different microstructures of M-NiAl are very complex, as described in related work [10, 11]. Our detailed research will be reported in a future paper [12]. Hence, it can be seen that both sizes of the grains and substructures of M-NiAl in Ni–34.6 at % Al were all substantially refined after rapid solidification and following solid-state quenching at very high speeds. Moreover, the sizes of the grains and substructures decreased with increasing cooling rates.

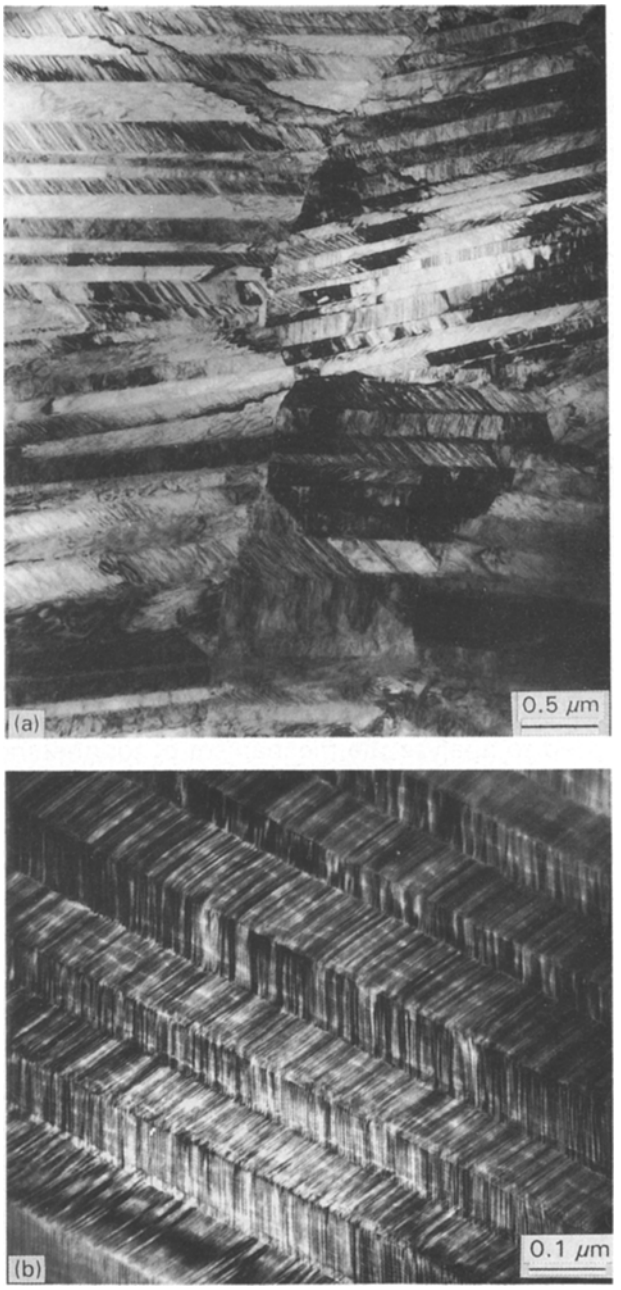

Figure 1 Transmission electron micrographs of M-NiAl in Ni–34.6 at % Al: (a) M-NiAl with complex substructures, (b) M-NiAl twins with very fine size.

3.2. Reaction between propagating microcracks and interfaces

Refining the sizes of grains and substructures of M-NiAl resulted in many interfaces of different types with high density and homogeneous distribution, including grain boundaries, interfaces between variants, twin or stacking fault plates, secondary twin or stacking fault plates. It was found that the interfaces effectively resisted microcrack propagation, which was probably induced by the thermal stress during rapid solidification and quenching, and deflection, twisting and branching of the microcracks resulted. Fig. 3 shows a deflected microcrack propagating from the left to the right across two grains. It can be seen in Fig. 3a that the propagating direction of the microcrack changed at least three times within the left-hand grain and each change in propagation direction occurred at the interfaces between the twin plates. After the microcrack crossed the grain boundary, it zigzagged then branched into two similar zigzag submicrocracks and stopped at the end, which is more apparent in Fig. 3b. The small change in propagation direction within one twin plate suggests that even the interfaces between the secondary twin or stacking fault plates played an effective resistant role against microcrack propagation and made a contribution to the toughening of NiAl. Fig. 4 shows another similar zigzag and twisted microcrack. It can be seen that a shear displacement parallel to the general direction of propagation of the microcrack occurred between the two parts of the twin plates separated by the propagating microcrack. The displacement decreased gradually along

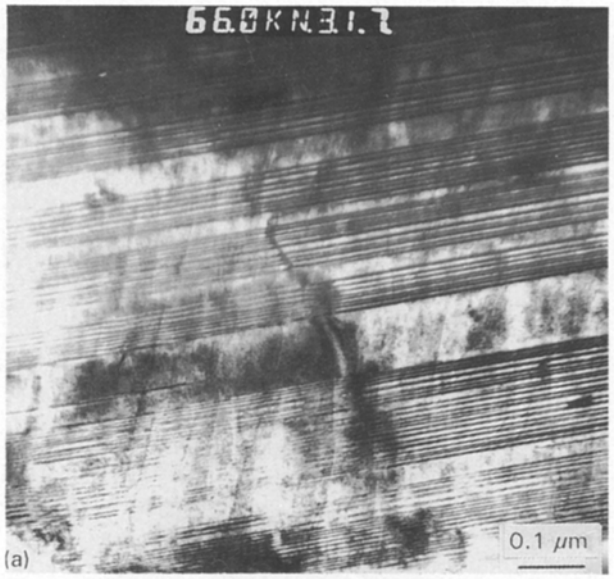

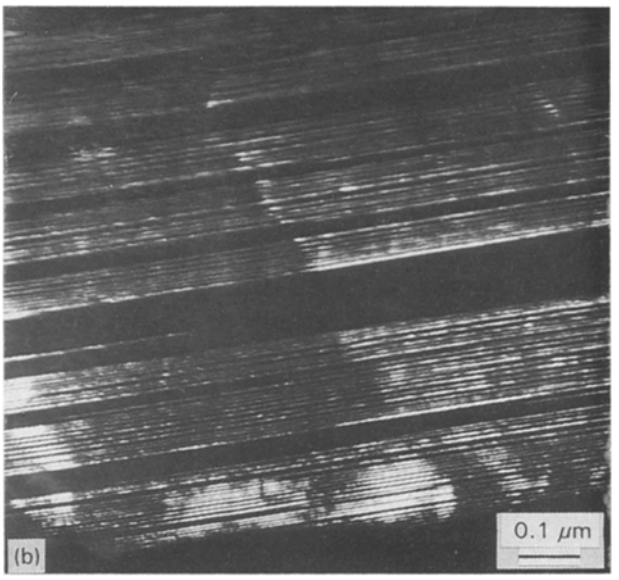

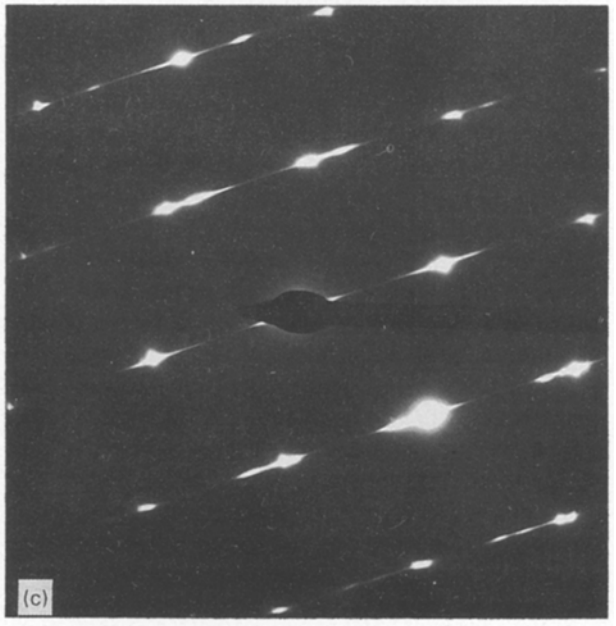

Figure 2 Transmission electron micrographs of M-NiAl twins in Ni–34.6 at % Al: (a) bright field, (b) dark field, (c) selected-area electron diffraction pattern of (a), $L1_0$ {0 1 1} zone.

the direction of propagation, indicating that considerable energy was dissipated when the microcrack crossed through the interfaces between the twin plates, similar to the limited debonding during crack bridging in composites, which can enhance toughening [13]. Furthermore, a localized plastic deformation and emission of dislocation arrays were observed ahead of the tips of the microcracks when they crossed through the interfaces, as shown in Fig. 5. Through localized plastic deformation, the stress at the tip of the microcrack was relaxed; therefore, the tip was blunted and the microcrack was prevented from propagating further. Moreover, it is easy to see that, in addition to the larger zigzag microcrack, several other smaller microcracks also nucleated in most cases at the interfaces between twin plates, and a few dislocations were emitted. This suggests that the localized plastic deformation in fine-grained NiAl can not only occur during microcrack nucleation at the interfaces, but can also take place during crack propagation when they were resisted by the interfaces. Fig. 6 shows scanning electron micrographs of bent fracture surfaces and the adjacent area of the top surface of ribbon N-1. They provide further evidence of plastic deformation over a larger range before fracture. The thickness in the centre of the ribbon in Fig. 6a was very small, only about 1 μm. The reason for the occurrence of this situation is not yet clear. However, it can be seen that only the central area of the sample had substantially undergone necking before fracture and the protuberance was very similar to the shear lip in the tensile fracture surface with good plasticity. Near the protuberance, parallel slip bands or lines which delineated the intersections of active slip planes and the surface of the ribbon, can be observed in several places (Fig. 6b). On considering the relations between the cooling rate and thickness of melt-spun ribbons, as well as that between the cooling rate and grain size [14], it can be deduced that the sizes of the grains and substructures in this region must be particularly fine. In fact, the size of some equiaxed grains appearing on the top surface of the ribbon is only about 0.2 μm (Fig. 6b), which is much smaller than the critical grain size calculated by Chan [6], even considering the effect of non-stoichiometry on the critical grain size [3], so that the occurrence of plastic deformation in the larger region is not surprising.

Most of all, the above experimental results indicate that refining the microstructures of Ni–34.6 at % Al increased the concentration of interfaces with different types and with homogeneous distribution. The interfaces as well as grain boundaries, effectively resisted microcrack propagation and resulted in localized plastic deformation, sometimes in larger regions. This must improve the ductility and toughness at room temperature of the nickel-rich NiAl. The study of microstructures and the results are very consistent with the results of bend ductility [9] and the comparative observation of fracture surfaces between the cast alloy and ribbons in the Ni–34.6 at % Al [7]. The bend strain to failure of ribbon N-1 is about three times larger than that of ribbon N-3. The toughness of

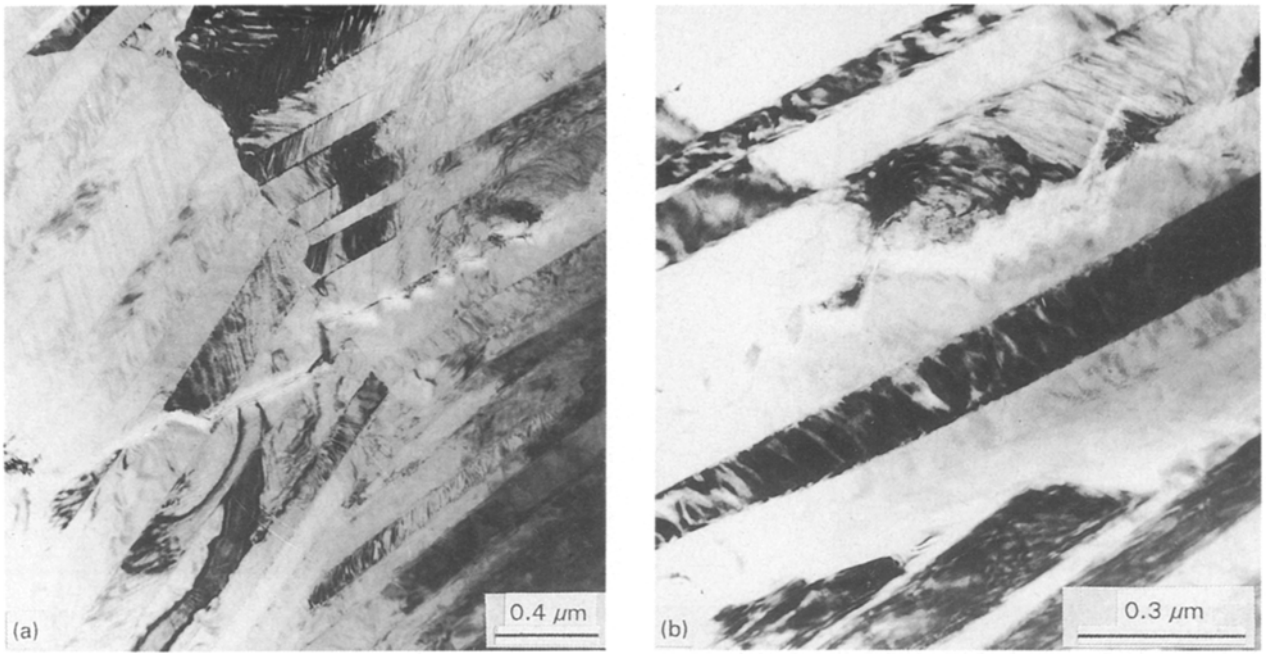

Figure 3 Transmission electron micrographs of a deflected and branched microcrack in Ni–34.6 at % Al: (a) low magnification, (b) higher magnification.

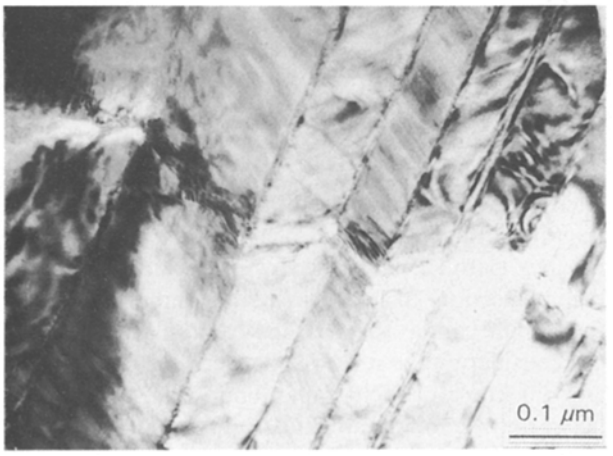

Figure 4 Transmission electron micrograph of the reaction between the twisted microcrack and interfaces in Ni–34.6 at % Al.

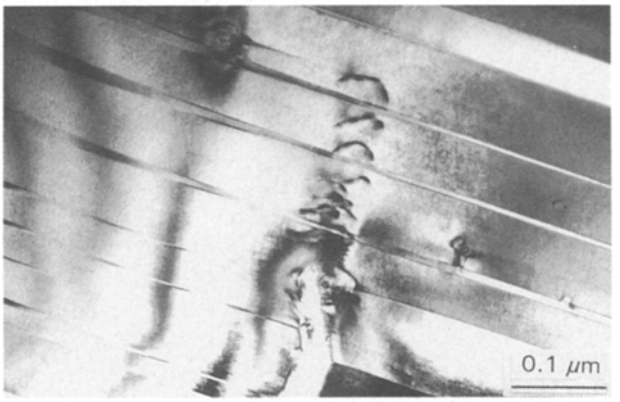

Figure 5 Transmission electron micrograph of the emission of dislocations at the tips of the microcracks and tip blunting.

the ribbons also was considerably improved and some thinner samples of ribbons N-1 and N-2 can be bent to 180° without failure.

4. Discussion

4.1. Mechanism of improving the ductility

Owing to strong directional bonding [15], the very high ordered energy leading to the poor dislocation mobility and insufficiently independent slip systems in NiAl [1], the stress concentration and subsequent nucleation of cracks at the interfaces, such as grain boundaries, occur easily when the external stress reaches a certain level. Hence, there are at least two ways to improve the toughness of NiAl at room temperature. One way is by diminishing the stress concentration at the interfaces so that the nucleation of cracks can be suppressed to some extent. The other way is by raising the crack resistance in order to avoid or delay unstable crack propagation. It is apparent that both ways can be achieved by refining microstructures or increasing the density of interfaces. However, the more effective role of grain size reduction seems to enhance the crack resistance in brittle alloys such as NiAl, according to the above experimental results.

In general, the crack resistance accompanying the crack propagation includes mainly surface energy, plastic deformation work and dissipated energy resulting from the reaction between interfaces and the propagating crack, especially microcracks [16]. It is clear that the magnitude of the plastic deformation work in crack propagation is a very important factor in determining the types of fracture, i.e. ductile or brittle, and the ductility of the alloys. In brittle materials there is no doubt that the difficulty in the production of dislocations, poor mobility of the dislocations and the low number of active slip systems at ambient temperature, are the main reasons for their bad ductility. However, based on above experimental results, it

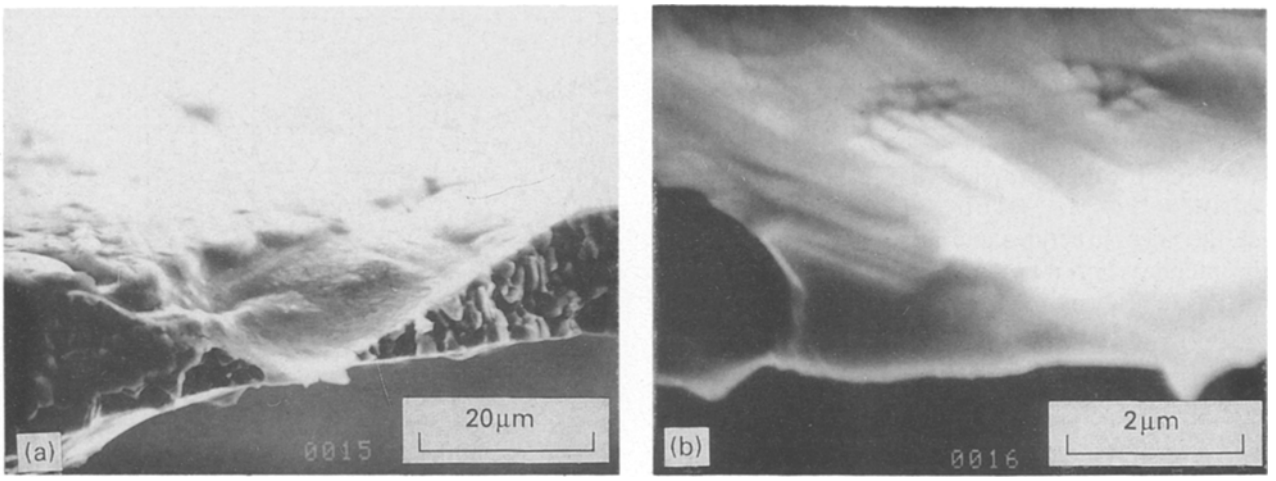

Figure 6 Scanning electron micrographs of plastic deformation near the fracture surfaces in Ni–34.6 at % Al: (a) protuberance in the middle of the sample, (b) slip bands and lines in the same region, at higher magnification.

can still be deduced whether the plastic deformation resulting to some extent before unstable propagation of the crack also depends closely on the stress distribution, or on the extent of stress concentration. When the sizes of grains and other substructures are larger, the density of the interfaces is low and the distribution of the interfaces is usually inhomogeneous so the stress distribution is also inhomogeneous under a certain external stress. Correspondingly, the stress concentration at fewer interfaces must be severe, where a sharp crack instead of zigzagged microcracks is easy to nucleate. Hence, with increasing external stress, the extent of stress concentration in the few regions where the cracks have already nucleated, rapidly becomes more severe, so the crack propagation driving force becomes great. It is probable that insufficient time is available to result in localized plastic deformation before the unstable and very fast propagation of the cracks. The factor is perhaps more dominant for the emission of dislocations in NiAl because the dislocations resulting from crack-tip emission in intermetallics with the B2 structure are usually complex and dissociated superlattice dislocations [17]. In fact, because a certain time is necessary for the emission and motion of the dislocations, Tatelman and Robertson [18] found the following relation between the plastic deformation work, w_p, and the speed of crack propagation, V_c, during crack propagation

$$W_p/\gamma_0 = cs_0^{3/2}\boldsymbol{b}^3(V_0/V_c)^2T^{5/2} \quad (1)$$

where γ_0 is the specific surface energy, s_0 the density of dislocation sources, $\boldsymbol{b}$ is Burgers vector, V_0 the speed of the elastic wave, T the temperature, and c is a constant. It is evident that the plastic deformation work, W_p, is larger compared with γ_0 at room temperature, only when the speed of crack propagation, V_c, is smaller, if s_0 and $\boldsymbol{b}$ are constant. Moreover, when the sizes of the grains and other substructures are larger and the density of interfaces is smaller, the brittleness of the interfaces, especially the grain boundaries, resulting from segregation of the impurities, poor bonding, defects, etc., is very prominent. In other words, the difference in the microplasticity [19] or microtoughness between the interfaces and matrix is great. Hence, it is easy and preferential that the crack propagates along the grain boundaries or other interfaces, when the external stress is enhanced. It must again promote the unstable propagation of the crack because it is almost impossible to result in localized plastic deformation ahead of the cracks along the interfaces. The plastic deformation work in this situation almost equals zero and the crack resistance is also very small, therefore brittle fracture finally results, as observed in the traditionally cast NiAl [7].

In the opposite situation, when the sizes of the grains and other substructures are significantly refined, the density of the interfaces with different types increases and its distribution is homogeneous. The stress distribution also becomes more homogeneous and the stress concentration is smoothed so microcracks may nucleate at the interfaces after localized plastic deformation to some extent, as shown in Fig. 5, which can again smooth the stress concentration. Propagating microcracks with deflection, bowing, twisting and branching, usually result at many interfaces, as shown in Figs 3 and 4, which can shield or diminish the stress concentration around the microcracks [20]. The nucleation of the main crack is probably delayed or even avoided, when the external stress is enhanced. Hence, the change in the extent of stress concentration around the tips of each microcrack is then slower with increasing external stress, and the time available for localized plastic deformation ahead of the tips of the microcracks would be more sufficient even for plastic deformation in larger regions, as shown in Figs 5 and 6. It was recently reported that dislocation emission from the tips of propagating microcracks and tip blunting are the key factors leading to ductile fracture in brittle intermetallics with the B2 structures [17]. Moreover, interface brittleness or difference of bonding characteristics between the interfaces and the matrix would be reduced with increasing density of interfaces. Thus, the percentage of intrafacial propagation of the microcracks increases, as observed in Figs 3 and 4, as well as fracture surfaces

[7], which also promotes localized plastic deformation ahead of the tips of the microcracks. Furthermore, it is evident that refining the grain size also enhances the probability of the occurrence of grains with the soft orientation under a certain external stress, because the slip system in NiAl is predominantly $<100>\{100\}$ or $<100>\{110\}$ [1]. Thus, refining the microstructures and increasing the density of the interfaces in NiAl provide the necessary conditions for plastic deformation to some extent, so not only the ductility can be improved but also a large contribution of the plastic deformation work can be made to the crack resistance or improvement of toughness.

4.2. Simplified model of toughening NiAl

As mentioned above, surface energy is also one part of the crack resistance during crack propagation; it increases proportionally with increasing total length of the crack, including the microcracks; therefore, deflection, bowing, twisting and branching of the cracks all increase the surface energy. On the other hand, when a microcrack crosses an interface, the impingement and friction between the microcrack and interfaces must dissipate much energy, as shown in Figs 3 and 4, which is closely associated with the length of the crack and the density of the interfaces. In order to study further the effects of refining microstructures or increasing the interface density on the toughness of NiAl, a simplified model is presented, based on the above experimental results and analysis, and is graphically shown in Fig. 7. It is simply assumed that the interfaces in a ribbon with unit thickness are parallel and equidistant from each other. The model concentrates on the reaction between the interfaces and intrafacially propagating microcrack. The total energy required, U_1, when the microcrack shown in Fig. 7 propagates over a length a along the direct line OCA, can be approximately indicated as

$$U_1 = 2f_1(a)\gamma_0 + F_1(a)U_{01}/d_1 + G\{[(a/d_1)n_1\boldsymbol{b}]^2/4\pi(1-\nu)\}\ln(R/\gamma) \quad (2)$$

where d_1 is the distance between the interfaces, U_{01} is the average dissipated energy owing to impingement and friction between the microcrack and the interfaces when the microcrack grows through each interface, $f_1(a)$ and $F_1(a)$ are functions of the length and depth of the propagating microcrack, which indicate, respectively, the dependent relations of surface energy and dissipated energy on the geometric features of the microcrack, G is the shear modulus, n_1 the average number of emitted dislocations of Burgers vector $\boldsymbol{b}$ from the tip of the microcrack during its growth over a distance d_1, ν is Poisson's ratio, R is the effective radius of the stress field of the dislocation, and r is its core radius. It is clear that the terms on the right-hand side of Equation 2 correspond to the surface energy, dissipated energy and energy of dislocation emission or plastic deformation work, respectively.

When the microstructures are substantially refined and the distance between the interfaces decreases, deflection and twisting of the microcracks are most likely to take place, as discussed before. If the deflection or twisting angle, θ, is assumed to be constant, as shown in Fig. 7, when the microcrack extends over the same distance a along a zigzag line OBCDA instead of OCA, and $\ln(R/r)$ in the third term of Equation 2 is simplified to 4π [21], then the total energy for microcrack propagation should be

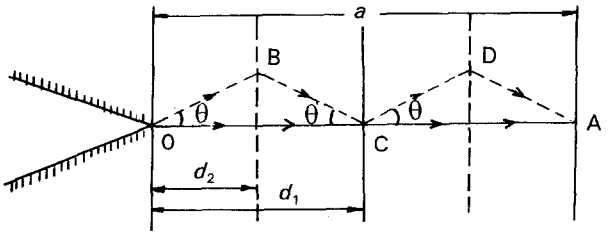

Figure 7 Schematic illustration of the reaction between the propagating microcrack and interfaces.

$$U_2 = 2f_2(a)\gamma_0/\cos\theta + F_2(a)U_{02}/d_2 + G(an_2\boldsymbol{b})^2/(1-\nu)\,d_2^2 \quad (3)$$

where subscript 2 refers the deflected or twisted microcrack.

At the same time, assuming that the slip band has formed and crossed the distance between neighbouring interfaces, the relation between the effective shear stress on the slip plane $(\tau - \tau_0)$, where τ is the applied shear stress and τ_0 is the internal friction stress required to overcome resistance for dislocation motion [21], and plastic displacement $n\boldsymbol{b}$ is

$$(\tau - \tau_0)/G = n\boldsymbol{b}/d \quad (4)$$

therefore

$$n\boldsymbol{b} = (\tau - \tau_0)\,d/G \quad (5)$$

For the condition where localized plastic deformation occurs ahead of the tip of the microcrack, $(\tau - \tau_0)$ can be approximately replaced by $K_y d^{-1/2}$ where (K_y is a constant) from the Hall–Petch equation [21], and Equation 5 is then

$$n\boldsymbol{b} = K_y d^{1/2}/G \quad (6)$$

so Equation 3 can be rewritten as

$$U_2 = 2f_2(a)\gamma_0/\cos\theta + F_2(a)U_{02}/d_2 + K_y^2 a^2/(1-\nu)Gd_2 \quad (7)$$

Hence, if the number of branches of the microcrack is m, the crack resistance, R_1 [16], for a deflected, twisted and branched microcrack as shown in Fig. 3 is

$$R_1 = \mathrm{d}U_2/\mathrm{d}a = \sum_{i=1}^{m}\{2f'_2(a_i)\gamma_0/\cos\theta_i + F'_2(a_i)U_{0i}/d_2 + 2K_y^2 a_i/(1-\nu)Gd_2\} \quad (8)$$

where $f'_2(a_i)$ and $F'_2(a_i)$ refer to $\partial f_2(a_i)/\partial a_i$ and $\partial F_2(a_i)/\partial a_i$, respectively. It is evident from Equation 8 that decreasing d_2 or increasing the density of the interfaces, increasing appropriately the deflection or twisting angle θ, enhancing the dissipated energy U_{0i}, increasing the number of branches of the microcrack, m, and the emission of the dislocations or plastic work, can all

raise the crack resistance, R_1, which are all related to refining microstructures. Hence, this proves that refining the microstructures is an important factor for increasing R_1 or improving the toughness of NiAl, which is consistent with above experimental results. In fact, comparing Equation 8 with the modified Griffith equation given by Irwin and Orowan [22] for incompletely brittle materials

$$R_1 = 2(\gamma + \gamma_p) \quad (9)$$

where γ is the surface energy and γ_p is the plastic deformation work accompanying the crack extension, it can be found that Equation 8 is a specific and more complete form of Equation 9. Moreover, the present model and Equation 8 can also be applied for bridged microcracks, if U_{0i} corresponds to that situation.

It should be mentioned that the other effect of microcrack propagation, in addition to increasing crack resistance, is the release of the elastic strain energy, U_e, around the microcrack. The elastic energy release rate, G_1, under the condition of plane stress for thin ribbons can be expressed as [16]

$$G_1 = dU_e/da = \pi\sigma^2 a/E \quad (10)$$

where σ is the external stress, E the elastic modulus. It is apparent that G_1 is closely associated with the extent of stress concentration and can be considered to be the crack-propagation driving force. In the situation of incompletely brittle fracture before the unstable extension, the crack resistance, R_1, is larger than G_1 or $R_1 = G_1$, but $\partial R_1/\partial a > \partial G_1/\partial a$, while G_1 is larger than R_1 only when unstable crack propagation occurs. It can be found qualitatively from Equations 8, 10 and the above analysis, that both R_1 and G_1 are affected by the extension of the crack or increasing the length of the crack, but R_1 is still determined by the size of the microstructures, such as grain size. Thus, when the size of the microstructures is larger, R_1 may be smaller than G_1 during the whole propagation of the crack under a certain external stress, which is the situation of brittle fracture. In the opposite case, when the size of the microstructures is small enough, R_1 would be larger than G_1, and the crack, including microcracks, extends stably, accompanying plastic deformation for a long way, and the final failure occurs only when the external stress is enhanced to the higher level. This is the situation of ductile fracture. Therefore, it is natural that there should be a critical size of microstructures, such as the critical grain size, which corresponds to $G_1 = R_1$ and $\partial R_1/\partial a = \partial G_1/\partial a$, or the change from brittle fracture to ductile fracture. The analysis of results is basically consistent with Schulson and Barker's [3] and Chan's [6] work, although they did not consider specifically the effects of refining grain size on crack propagation, which is very important for improving the ductility and toughness of NiAl as discussed above. Moreover, the idea of refining grain size is developed into refining the microstructure size in the present work, which expands the possible ways to improve the ductility and toughness of NiAl and other brittle intermetallics. However, it should be pointed that Equation 8, based on the energy balance calculation, is approximate and it is difficult to give accurate expressions of the functions $f(a)$ and $F(a)$ at this moment, so the critical size of the microstructures, d_c, was not derived from Equations 8 and 10. The different roles in improving the ductility and toughness of NiAl of different types of interfaces also need to be studied specifically. It is probable that a combined study employing continuous medium elastic mechanics [6, 19] and an investigation using the energy balance calculation based on interaction between the propagating crack and microstructures, would be the better approach to explore further the mechanism of toughening of NiAl by refining the microstructures.

Moreover, although refining the microstructures can improve both ductility and toughness of NiAl at room temperature, the effects of refined microstructures on high temperature properties, especially creep strength, should still be considered, because NiAl is a potential high-temperature structural material. Fine microstructures, e.g. fine grains, are normally disadvantageous for creep strength and other high-temperature properties. The NiAl martensite as a metastable phase can not be retained at high temperature either, although the important role of the interfaces in raising the crack resistance is universal, which may be useful for improving the ductility and toughness of two- or three-phase intermetallic alloys [22]. Hence, the questions remain of how to retain the refined microstructures up to higher temperature and how to change the negative effects of refined microstructures on the high-temperature properties of NiAl. One valuable answer is the development of nanometre intermetallics because a great change would occur in composition, structure, volume percentage and behaviour at high temperature of the interfaces in these alloys [23]. Of course, the large-scale manufacturing of nanometre alloys still remains a problem at this stage. The other choice is by manufacturing MMCs with a matrix of nanometre NiAl. If ceramic particles with good compatibility with NiAl can be homogeneously distributed on the matrix [9] and pin the interfaces at high temperature, this perhaps would be a better way to improve the properties of NiAl at room and high temperature at the same time [23]. It is evident that the present results and discussion of the positive effects of refining microstructures or increasing the density of the interfaces on improvement of the ductility and toughness of NiAl can be applied to the other brittle intermetallics, ceramics and materials.

5. Conclusions

1. In melt-spun Ni–34.6 at % Al ribbons with high cooling rates during rapid solidification and solid quenching, refining the sizes of NiAl martensite grains (average size down to 2.2 μm) and substructures (average size down to 8 nm) resulted in interfaces with a high density and homogeneous distribution, which can change the stress distribution and smooth the stress concentration.

2. The reaction between the extending microcracks and interfaces not only promoted plastic deformation in a local area ahead of the tips of the microcracks and

in larger regions with finer grains (about 2 μm), but also resulted in the deflection, branching, and twisting of the microcracks.

3. In terms of improving the ductility and toughness of NiAl at room temperature, the idea of refining the grain size was developed into refining the microstructure size. A simplified model of the reaction between the propagating microcracks and interfaces, based on the experimental results, is presented and the analysis suggests that refining microstructures below a critical size and increasing the density of the interfaces are the key factors for improving the ductility and toughness of NiAl at room temperature. The present results may be useful for improving the ductility and toughness of the other brittle materials.

Acknowledgements

The author thanks the K. C. Wong Foundation and the Royal Society for financial support, and Professor Sir Peter Hirsch and Dr. B. Cantor, University of Oxford, for provision of laboratory facilities. Professors M. McLean and H. M. Flower, Imperial College, are particularly thanked for provision of laboratory facilities and helpful discussion. This work was also supported by the Chinese Doctoral Program Fund of CEC.

References

1. R. DAROLIA, *J. Metals* **3** (1991) 44.
2. E. M. SCHULSON, *Res. Mech. Lett.* **1** (1981) 111.
3. E. M. SCHULSON and D. R. BARKER, *Scripta Metall.* **24** (1983) 519.
4. D. J. GAYDOSH, R. W. JECH and R. H. TITRAN, *J. Mater. Sci. Lett.* **4** (1985) 138.
5. E. M. SCHULSON, *Int. J. Powder Metall.* **1** (1987) 25.
6. K. S. CHAN, *Scripta Metall.* **24** (1990) 1725.
7. TIANYI CHENG, M. McLEAN and H. M. FLOWER, *ibid.* **26** (1992) 1913.
8. P. NAGPAL and I. BAKER, *ibid.* **24** (1990) 2381.
9. TIANYI CHENG, *ibid.* **27** (1992) 771.
10. K. ENAMI, S. NENNO and K. SHIMIZU, *Trans. JIM* **14** (1973) 161.
11. S. CHAKRAVORTY and C. M. WAYMAN, *Metall. Trans.* **7A** (1976) 569.
12. TIANYI CHENG, *Scripta Metall.*, submitted.
13. V. C. NARDONE and J. R. STRIFE, *Metall. Trans.* **22A** (1991) 183.
14. TIANYI CHENG and SHOUHUA ZHANG, "Rapid Solidification Technology and Advanced Alloys" (Chinese Aerospace, Beijing, 1990).
15. W. LIN, JIAN-HUA XU and FREEMAN, *J. Mater. Res.* **7** (1992) 592.
16. H. L. EWALDS and R. J. H. WANHILL, "Fracture Mechanics" (Edward Arnold, London, 1986).
17. M. F. BARTHOLOMEUSZ and J. A. WERT, *J. Mater. Res.* **7** (1992) 919.
18. A. S. TETELMAN and W. D. ROBERTSON, *Acta Metall.* **11**(1963) 1.
19. C. J. McMAHON Jr, "Microplasticity" (Wiley, New York, 1968).
20. K. T. FABER and A. G. EVANS, *Acta Metall.* **3** (1983) 565.
21. I. L. MAY, "Principle of Mechanical Metallurgy" (Edward Arnold, London, 1981).
22. S. SAMPATH, R. TINARI, B. GUDMUNDSSON and H. HERMAN, *Scripta Metall.* **25** (1991) 7425.
23. T. HAUBOLD, R. BOHN, R. BIRRINGER and H. GLEITER, *Mater. Sci. Eng.* **A153** (1992) 679.

Received 2 October 1992
and accepted 3 February 1993